How to cite: *Angew. Chem. Int. Ed.* **2023,** *62,* e202218350
International Edition: doi.org/10.1002/anie.202218350
German Edition: doi.org/10.1002/ange.202218350

Nanographenes

Synthesis of Bioctacene-Incorporated Nanographene with Near-Infrared Chiroptical Properties

Xiushang Xu, Rafael Muñoz-Mármol, Serhii Vasylevskyi, Andrea Villa, Giulia Folpini, Francesco Scotognella, Giuseppe Maria Paternò, and Akimitsu Narita**

Abstract: We report the synthesis of a hexabenzoperihexacene (HBPH) with two incorporated octacene substructures, which was unambiguously characterized by single-crystal X-ray analysis. The theoretical isomerization barrier of the (*P*,*P*)-/(*P*,*M*)-forms was estimated to be 38.4 kcal mol^{-1}, and resolution was achieved by chiral HPLC. Notably, the enantiomers exhibited opposite circular dichroism responses up to the near-infrared (NIR) region (830 nm) with a high g_{abs} value of 0.017 at 616 nm. Moreover, HBPH demonstrated NIR emission with a maximum at 798 nm and an absolute PLQY of 41 %. The excited-state photophysical properties of HBPH were investigated by ultrafast transient absorption spectroscopy, revealing an intriguing feature that was attributed to the rotational and/or conformational dynamics of HBPH after excitation. These results provide new insight into the design of chiral nanographene with NIR optical properties for potential chiroptical applications.

[*] X. Xu, A. Narita
Organic and Carbon Nanomaterials Unit, Okinawa Institute of Science and Technology Graduate University
1919-1 Tancha, Onna-son, Kunigami-gun, Okinawa 904-0495 (Japan)
E-mail: akimitsu.narita@oist.jp

R. Muñoz-Mármol, A. Villa, F. Scotognella, G. Maria Paternò
Physics Department, Politecnico di Milano, Piazza L. da Vinci 32, 20133 Milano (Italy)
E-mail: giuseppemaria.paterno@polimi.it

S. Vasylevskyi
Engineering Section, Research Support Division, Okinawa Institute of Science and Technology Graduate University
1919-1 Tancha, Onna-son, Kunigami-gun, Okinawa 904-0495 (Japan)

G. Folpini, G. Maria Paternò
Center for Nano Science and Technology, Istituto Italiano di Tecnologia
Via Pascoli 70, 20133 Milano (Italy)

A. Narita
Max Planck Institute for Polymer Research
Ackermannweg 10, 55128 Mainz (Germany)

Nanographenes (NGs) have attracted widespread attention because of their fascinating physicochemical properties, which can be drastically modulated by changing their size, shape, and especially edge structures.[1] In particular, the presence of zigzag edges, corresponding to acene substructures, imparts NGs with unique optoelectronic and magnetic properties,[2] such as relatively small energy gaps,[3] a high photoluminescence quantum yield (PLQY),[4] stimulated emission,[5] and open-shell di- to multiradical characteristics.[2,6] Periacenes, comprising two rows of *peri*-fused acenes, is one of the most intriguing classes of NGs with zigzag edges and have been targets of recent synthetic efforts.[6] In 2018, two groups independently described the synthesis of peritetracene, achieving its isolation and crystallization as well as revealing its open-shell biradical character and reactivity toward the Diels–Alder reaction at the bay regions, leading to circumanthracene.[7] Nevertheless, the preparation of peripentacene has been realized only on a metal surface under ultrahigh vacuum (UHV),[8] and periheptacene needs to be characterized in situ due to its low stability,[9] impeding its in-depth investigations and applications. To this end, the fusion of benzene rings at zigzag edges is known as a strategy to improve the stability,[10] and a dibenzoperihexacene (DBPH) derivative was isolated as a highly stable compound, showing red emission with maximum at 648 nm.[11] Unsubstituted DBPH and dibenzoperioctacene (DBPO) could be formed on metal surfaces under UHV, revealing energy gaps of ca. 2.1 and 1.3 eV, respectively, by scanning tunneling spectroscopy,[12] but this method does not allow the isolation of the products nor the scale up. To this end, synthesis and isolation of zigzag-edged NGs with incorporated biacenes higher than hexacene have remained a challenge.[10d]

In contrast to NGs with planar aromatic cores, nonplanar NGs with helical (sub)structures can exhibit chirality,[13] providing the opportunity for various potential applications, ranging from chiral optics[14] and chiral sensors[15] to asymmetric catalysis.[16] For example, NGs with fjord edges, corresponding to [5]helicene substructures, can be made chiral by the introduction of bulky substituents to prohibit racemization,[17] and a growing number of chiral NGs have also been obtained by incorporating higher helicenes.[18] Chiral NGs with absorbance and emission across the visible light region have thus been reported as potential chiroptical materials,[13a,16,19] and significant efforts have been recently devoted to realizing chiral NGs with near-infrared (NIR) optical properties. The extension of the

effective π-conjugation length of helical frameworks and the fusion of multiple helicenes to a large NG core can decrease the energy gap, enabling chiroptical responses in the NIR spectral range, but reported examples of such chiral NGs with NIR optical properties are still rare.[18d,20]

Herein, we report the synthesis and characterization of hexabenzoperihexacene (HBPH) as an unprecedented bioctacene-incorporated NG with zigzag edges, which exhibited NIR absorption and emission (Figure 1). Bulky *tert*-butyl groups were substituted onto the fjord edges to obtain chiral HBPH by enhancing the isomerization energy barrier.[17c,d] The X-shaped configuration of HBPH was revealed by X-ray crystallography, and resolution was achieved by chiral high-performance liquid chromatography (HPLC). The enantiomers of HBPH exhibited electronic circular dichroism in the visible to NIR regions (up to 830 nm) with a high dissymmetry factor (g_{abs}) value of 0.017 at 616 nm. Furthermore, HBPH displayed an emission maximum at 798 nm with an absolute photoluminescence quantum yield (PLQY) of 41 %, highlighting its great potential for chiral optoelectronic devices.

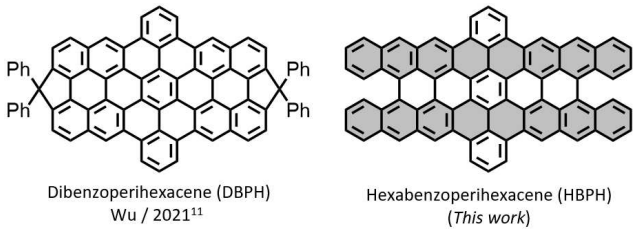

Figure 1. Chemical structure of dibenzoperihexacene (DBPH), and hexabenzoperihexacene (HBPH; this work). The substituents on the aromatic cores are omitted for clarity.

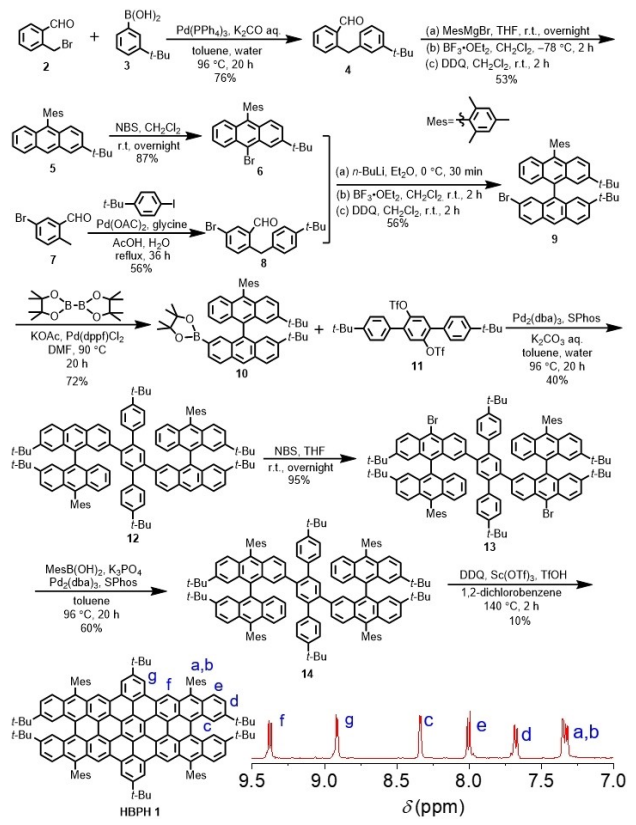

Figure 2. Synthetic route to HBPH **1** and the aromatic region of its ^{1}H NMR spectrum recorded in THF-d_8:CS_2 = 1:1 (500 MHz, 298 K).

For the synthesis of HBPH **1**, we designed precursor **14** based on the successful synthesis of dibenzo[a,m]dinaphtho[3,2,1-*ef*:1′,2′,3′-*hi*]coronene (DBDNC).[5c] 2-(3-*tert*-Butylbenzyl)benzaldehyde (**4**) was initially prepared by the Suzuki–Miyaura coupling of 2-bromomethylbenzaldehyde (**2**) and 3-*tert*-butylphenylboronic acid (**3**) with a 76 % yield (Figure 2). Subsequently, **4** was treated with 2-mesitylmagnesium bromide to provide a hydroxy intermediate, which was reacted with BF_3·OEt_2 and oxidized by 2,3-dichloro-5,6-dicyano-1,4-benzoquinone (DDQ) to afford 2-*tert*-butyl-10-mesitylanthracene (**5**) in 53 % yield. Then, 9-bromo-2-*tert*-butyl-10-mesitylanthracene (**6**) was produced via the bromination of **5** with *N*-bromosuccinimide (NBS) at room temperature with an 87 % yield. On the other hand, 5-bromo-2-(4-*tert*-butyl)benzylbenzaldehyde (**8**) was obtained by the palladium-catalyzed C(sp^3)–H activation reaction of 5-bromo-2-methylbenzaldehyde (**7**) and 4-*tert*-butyl-iodobenzene with a 56 % yield.[21] Then, **6** was lithiated and reacted with **8**. Subsequently, the obtained hydroxy intermediate was treated with BF_3·OEt_2 and oxidized by DDQ to afford 2-brominated 9,9′-bianthracene **9** with a 56 % yield. Subsequently, boronic ester **10** was obtained by the Miyaura-Ishiyama borylation of **9** with a 72 % yield. The Suzuki–Miyaura coupling of **10** and bitriflate **11** (see Supporting Information for the synthesis of **11**) afforded precursor **12** with a 40 % yield. The treatment of **12** with NBS afforded the dibrominated precursor **13** with a 96 % yield, followed by the Suzuki–Miyaura coupling with mesitylene-2-boronic acid to afford precursor **14** with a 60 % yield. Finally, the oxidative cyclodehydrogenation of **14** by using DDQ, scandium (III) triflate, and trifluoromethanesulfonic acid (TfOH) in 1,2-dichlorobenzene at 140 °C afforded HBPH **1** with a 10 % yield, the structure of which was unambiguously confirmed by the single-crystal X-ray analysis (see below). A well-resolved NMR spectrum of HBPH **1** was recorded at room temperature (Figure 2), and all the proton resonances were assigned based on ^{1}H-^{1}H COSY and NOESY techniques (see the Supporting Information). The observation of two separate peaks for each of the proton f, g, and c is most probably due to the presence of HBPH **1** both in racemic and *meso* forms.

The single-crystal of HBPH **1** was grown through the slow evaporation of its solution in hexane/CH_2Cl_2, enabling single-crystal X-ray analysis.[22] The HBPH **1** structure was clearly revealed with a planar dibenzoperihexacene core and nonplanar fjord edges (Figure 3). With the presence of bulky *tert*-butyl groups on the fjord edges, the torsion angle between the two rings was determined to be approximately 50.0° (Figure S25a), and the vertical distance of the centroid of the ring was estimated to be approximately 2.4 Å (Figure 3b). In a one-unit cell, the (*P*,*P*) and (*M*,*M*) enantiomers were stacked in an alternating manner along the *b*-axis with intermolecular distances of approximately

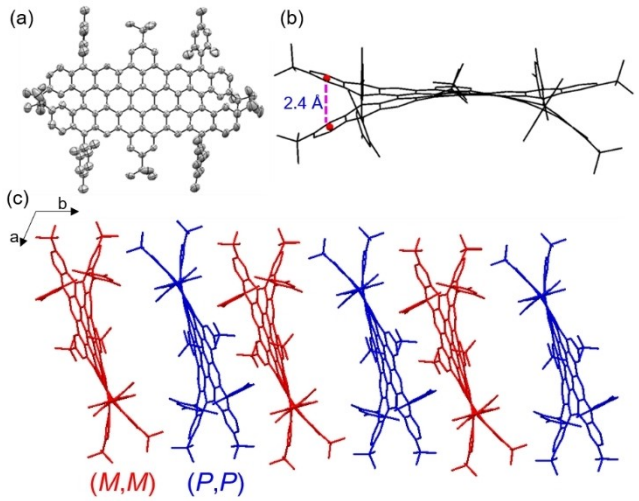

Figure 3. Single-crystal structure of HBPH **1**: a) front view (ellipsoids are shown at the 50% probability level), b) side view, and c) packing arrangement of HBPH **1** in the crystal (hydrogen atoms and solvents are omitted for clarity).

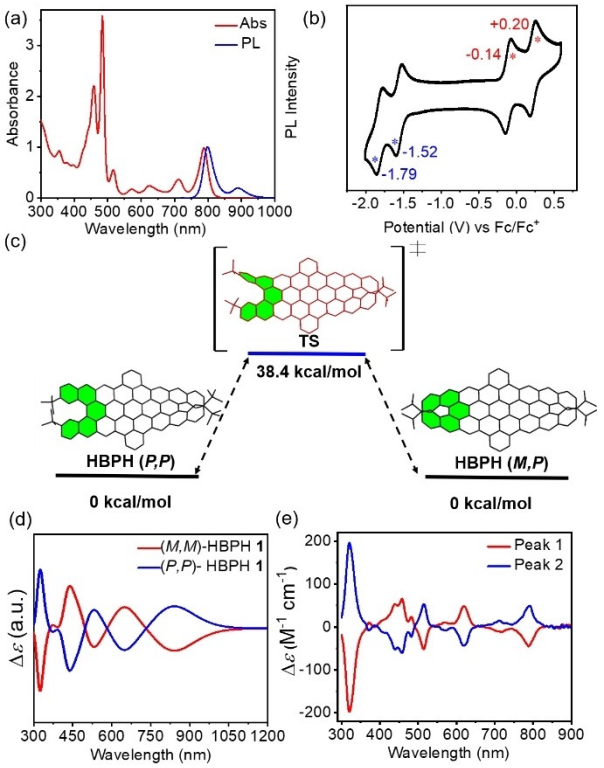

Figure 4. a) Normalized absorption and fluorescence spectra of HBPH **1** in toluene solution (10^{-5} M). b) Cyclic voltammogram of HBPH **1** in CH_2Cl_2 (5×10^{-4} M) with *n*-Bu_4NPF_6 (0.1 M) as the electrolyte, with the values of the half-wave potentials. c) Isomerization process of HBPH **1**. The relative Gibbs free energy (kcal mol^{-1}) was calculated at the B3LYP/6-311G(d,p) level. d) Simulated circular dichroism spectra of (*P*,*P*)-/(*M*,*M*)-HBPH **1** by TD-DFT at the PBE0/6-311G(d,p) level. e) Circular dichroism spectra of toluene solutions of **1** (10^{-5} M) obtained as the first and second peaks from the chiral HPLC separation.

7.4 Å, indicating their rather loose packing with an absence of strong π-π interactions. Additionally, the nucleus-independent chemical shift (NICS)[20a,23] and anisotropies of the induced current density (ACID)[24] of HBPH **1** were calculated, indicating the diatropic ring currents (red color) for the zigzag and fjord edges and strong local aromaticity in the fjord region (Figures S29–S30).

The absorption spectrum of HBPH **1** in toluene revealed a broad absorption band from the visible light to NIR region with three absorption maxima at 787 nm, 483 nm, and 458 nm (Figure 3a), which is in good agreement with time-dependent density functional theory (TD-DFT) calculations, e.g., the prediction of the HOMO→LUMO transition at 839 nm (Figure S31). The negligible change in the absorption spectrum of a solution of **1** after storage for 10 days in the dark under air at room temperature indicated its high stability (Figure S33). The emission spectra of HBPH **1** displayed maxima at 798, with small Stokes shifts of 11 nm (175 cm^{-1}), indicating its high structural rigidity. The optical energy gap was estimated to be 1.56 eV from the interface of the absorption and emission spectra. This value was consistent with the electrochemical energy gap of 1.33 eV calculated from the onset of the first oxidation and reduction peaks in its cyclic voltammogram (Table S4), which displayed two reversible oxidation and reduction peaks (Figure 4b). Remarkably, HBPH **1** showed a relatively high PLQY of ≈41 % in comparison to other NGs with NIR emission.[18d,20]

We estimated the isomerization barrier of HBPH with four *t*-Bu groups at the fjord regions to be 38.4 kcal mol^{-1} based on DFT calculations, which prompted us to resolve the two enantiomers of HBPH **1**. The resolution of (*P*,*P*)-/(*M*,*M*)-HBPH **1** was achieved via chiral HPLC using a Daicel Chiralpak IG column. Notably, the CD spectra of (*M*,*M*)-HBPH **1** in the ultraviolet, visible and NIR regions with $\Delta\varepsilon = 197\ M^{-1}cm^{-1}$ at 318 nm, $\Delta\varepsilon = -61\ M^{-1}cm^{-1}$ at 457 nm, $\Delta\varepsilon = -43\ M^{-1}cm^{-1}$ at 619 nm, and $\Delta\varepsilon = -43\ M^{-1}cm^{-1}$ at 789 nm were observed. Moreover, the maximum absolute dissymmetry factor $|g_{abs}|$ ($g_{abs} = \Delta\varepsilon/\varepsilon$) value of (*M*,*M*)-HBPH **1** reached 0.017 (616 nm) and 0.006 (770 nm), respectively, which might be related to its X-shaped conformation.[25] The simulated CD spectra were in good agreement with the experimental results, and the first and second peaks were assigned to (*M*,*M*)-HBPH **1** and (*P*,*P*)-HBPH **1**, respectively (Figures 4d and e, S31). The theoretical dissymmetry factor $|g_{cal}|$ was estimated to be 0.020 and 0.004 for the $S_0 \rightarrow S_3$ and $S_0 \rightarrow S_1$ transitions, respectively (Table S1), which is consistent with the experimental results.[13a]

Ultrafast transient absorption (TA) spectroscopy was used to explore the excited-state photophysical properties of HBPH **1** (Figure 5). The transient spectra displayed two main features: a positive peak at 795 nm that might be attributed to ground state photobleaching (PB) along with some stimulated emission (SE; 0′→0), and a negative peak at 725 nm associated with excited-state absorption (ESA). The temporal evolution of these two features showed an initial rise at 1 ps associated with internal conversion toward

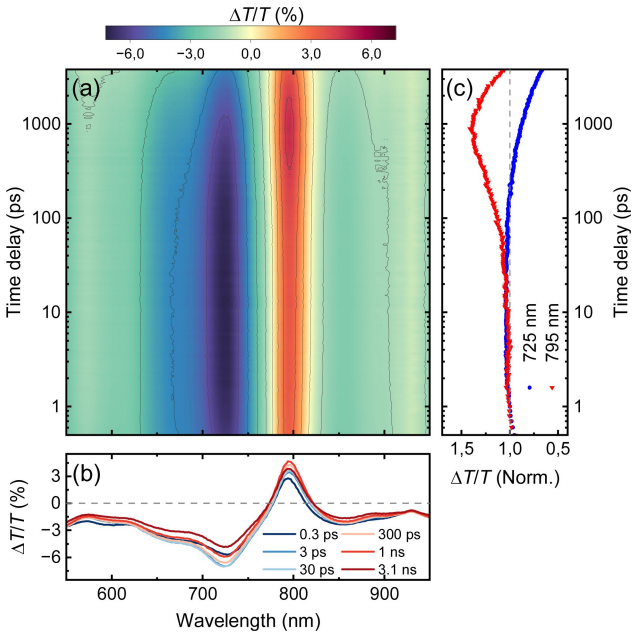

Figure 5. a) Differential transmission ($\Delta T/T$) map of HBPB 1 in toluene (0.1 mg mL^{-1}) under a 515 nm pump as a function of wavelength and time delay. b) $\Delta T/T$ spectra at various time delays. c) Time traces at 725 nm (blue circles) and 795 nm (red triangles) probe wavelengths. The pump wavelength and energy density were 515 nm and 85 μJ cm^{-2} (330 Hz), respectively.

the first excited state S_1, but the dynamics were dominated by a decay on the 10 ns timescale accounting for the decay back to the ground state, which was also supported by ns-TA measurements (Figure S35). Additionally, the peak at 795 nm exhibited a rise within the 400 ps timescale, providing evidence of the existence of an overlapped ESA feature with faster decaying dynamics than the $S_1 \rightarrow S_0$ transition. This rise was suppressed when HBPH **1** was dispersed in a polystyrene thin film to restrain the movement of the molecules (Figure S36), suggesting that this signature could be attributed to the rotational and/or conformational dynamics of HBPH **1** after excitation.[26]

The negative broad band of ESA convoluted with the full spectrum was attributed to the low energy gap combined with the high number of vibrational modes typical of large conjugated molecules.[27] Nevertheless, a small SE feature was found at approximately 890 nm, matching the second vibronic band of the PL. Interestingly, HBPH **1** displayed a more long-lived SE compared to previously reported NGs, such as DBOV-Mes-C12[5b] and DBDNC[5c] (Figure S37), although the overlap with the ESA quenched the SE, hampering the achievement of net optical gain. Similar results were obtained with lower concentrations of HBPH **1** and under pumping at 788 nm, suggesting the absence of significant contributions from intermolecular interactions or effects dependent on the excitation wavelength (Figures S38 and S39).

In summary, we synthesized HBPH **1** as a novel chiral and zigzag-edged NG with an incorporated bioctacene structure, whose X-shaped structure was confirmed by single-crystal X-ray diffraction. HBPH **1** exhibited a narrow optical energy gap (1.56 eV) and strong NIR emission with a high PLQY of 41 %. Moreover, strong chiroptical responses from 300 to 830 nm were revealed, with a high g_{abs} value (0.017). These results demonstrate the critical effect of the zigzag edges on the optoelectronic properties of chiral graphene nanoribbons (GNRs), indicating potential applications in chiral optoelectronic devices. Future efforts will also be directed to functionalize HBPH **1** with other chromophores, for example, fluoranthene imide (FAI),[26] which is expected to increase the conformational flexibility, leading to a larger Stokes shift and stabilization of the excited state to achieve net optical gain in the NIR.

Acknowledgements

This work was financially supported by the Okinawa Institute of Science and Technology Graduate University (OIST), JSPS KAKENHI Grant No. JP19K24686, and the European Union's Horizon 2020 Research and Innovation program under grant agreement no. 101017821 (LIGHT-CAP). G.M.P. thanks Fondazione Cariplo (Grant no. 2018-0979) for financial support. We appreciate the help and support provided by the Instrumental Analysis Section and the Scientific Computing and Data Analysis Section of Research Support Division at OIST.

Conflict of Interest

The authors declare no conflict of interest.

Data Availability Statement

The data that support the findings of this study are available from the corresponding author upon reasonable request.

Keywords: Chirality · Fjord-Edge · Nanographene · Near-Infrared · Zigzag-Edge

[1] a) A. Narita, X. Y. Wang, X. L. Feng, K. Müllen, *Chem. Soc. Rev.* **2015**, *44*, 6616–6643; b) M. Grzybowski, B. Sadowski, H. Butenschön, D. T. Gryko, *Angew. Chem. Int. Ed.* **2020**, *59*, 2998–3027; *Angew. Chem.* **2020**, *132*, 3020–3050; c) K. P. Loh, S. W. Tong, J. Wu, *J. Am. Chem. Soc.* **2016**, *138*, 1095–1102; d) S. Fujii, T. Enoki, *Acc. Chem. Res.* **2013**, *46*, 2202–2210; e) I. Pozo, E. Guitián, D. Pérez, D. Peña, *Acc. Chem. Res.* **2019**, *52*, 2472–2481; f) Y. Gu, Z. Qiu, K. Müllen, *J. Am. Chem. Soc.* **2022**, *144*, 11499–11524.

[2] a) J. Z. Liu, X. L. Feng, *Angew. Chem. Int. Ed.* **2020**, *59*, 23386–23401; *Angew. Chem.* **2020**, *132*, 23591–23607; b) W. D. Zeng, J. S. Wu, *Chem* **2021**, *7*, 358–386.

[3] J. E. Anthony, *Angew. Chem. Int. Ed.* **2008**, *47*, 452–483; *Angew. Chem.* **2008**, *120*, 460–492.

[4] a) Q. Chen, S. Thoms, S. Stöttinger, D. Schollmeyer, K. Müllen, A. Narita, T. Basché, *J. Am. Chem. Soc.* **2019**, *141*, 16439–16449; b) Y. W. Gu, X. J. Wu, T. Y. Gopalakrishna, H.

Phan, J. S. Wu, *Angew. Chem. Int. Ed.* **2018**, *57*, 6541–6545; *Angew. Chem.* **2018**, *130*, 6651–6655.
[5] a) V. Bonal, R. Muñoz-Mármol, F. G. Gámez, M. Morales-Vidal, J. M. Villalvilla, P. G. Boj, J. A. Quintana, Y. Gu, J. Wu, J. Casado, M. A. Díaz-García, *Nat. Commun.* **2019**, *10*, 3327; b) G. M. Paternò, Q. Chen, X. Wang, J. Liu, S. G. Motti, A. Petrozza, X. Feng, G. Lanzani, K. Müllen, A. Narita, F. Scotognella, *Angew. Chem. Int. Ed.* **2017**, *56*, 6753–6757; *Angew. Chem.* **2017**, *129*, 6857–6861; c) X. Xu, G. Serra, A. Villa, R. Muñoz-Mármol, S. Vasylevskyi, M. Gadea, A. Lucotti, Z. Lin, P. G. Boj, R. Kabe, M. Tommasini, M. Á. Díaz-García, F. Scotognella, G. M. Paternò, A. Narita, *Chem. Sci.* **2022**, *13*, 13040–13045.
[6] M. R. Ajayakumar, J. Ma, X. L. Feng, *Eur. J. Org. Chem.* **2022**, e202101428.
[7] a) M. R. Ajayakumar, Y. B. Fu, J. Ma, F. Hennersdorf, H. Komber, J. J. Weigand, A. Alfonsov, A. A. Popov, R. Berger, J. Z. Liu, K. Müllen, X. L. Feng, *J. Am. Chem. Soc.* **2018**, *140*, 6240–6244; b) Y. Ni, T. Y. Gopalakrishna, H. Phan, T. S. Herng, S. F. Wu, Y. Han, J. Ding, J. S. Wu, *Angew. Chem. Int. Ed.* **2018**, *57*, 9697–9701; *Angew. Chem.* **2018**, *130*, 9845–9849.
[8] C. Rogers, C. Chen, Z. Pedramrazi, A. A. Omrani, H.-Z. Tsai, H. S. Jung, S. Lin, M. F. Crommie, F. R. Fischer, *Angew. Chem. Int. Ed.* **2015**, *54*, 15143–15146; *Angew. Chem.* **2015**, *127*, 15358–15361.
[9] M. R. Ajayakumar, J. Ma, A. Lucotti, K. S. Schellhammer, G. Serra, E. Dmitrieva, M. Rosenkranz, H. Komber, J. Z. Liu, F. Ortmann, M. Tommasini, X. L. Feng, *Angew. Chem. Int. Ed.* **2021**, *60*, 13853–13858; *Angew. Chem.* **2021**, *133*, 13972–13977.
[10] a) H. M. Duong, M. Bendikov, D. Steiger, Q. C. Zhang, G. Sonmez, J. Yamada, F. Wudl, *Org. Lett.* **2003**, *5*, 4433–4436; b) M. Müller, S. Maier, O. Tverskoy, F. Rominger, J. Freudenberg, U. H. E. Bunz, *Angew. Chem. Int. Ed.* **2020**, *59*, 1966–1969; *Angew. Chem.* **2020**, *132*, 1982–1985; c) X. Yang, F. Rominger, M. Mastalerz, *Angew. Chem. Int. Ed.* **2021**, *60*, 7941–7946; *Angew. Chem.* **2021**, *133*, 8020–8025; d) Y. Gu, V. Vega-Mayoral, S. Garcia-Orrit, D. Schollmeyer, A. Narita, J. Cabanillas-González, Z. Qiu, K. Müllen, *Angew. Chem. Int. Ed.* **2022**, *61*, e202201088; *Angew. Chem.* **2022**, *134*, e202201088; e) Y. Zou, V. Bonal, S. M. Quintero, P. G. Boj, J. M. Villalvilla, J. A. Quintana, G. W. Li, S. F. Wu, Q. Jiang, Y. Ni, J. Casado, M. A. Diaz-Garcia, J. S. Wu, *Angew. Chem. Int. Ed.* **2020**, *59*, 14927–14934; *Angew. Chem.* **2020**, *132*, 15037–15044.
[11] Y. Zou, Y. Han, S. F. Wu, X. D. Hou, C. H. E. Chow, J. S. Wu, *Angew. Chem. Int. Ed.* **2021**, *60*, 17654–17663; *Angew. Chem.* **2021**, *133*, 17795–17804.
[12] Q. Zhong, Y. Hu, K. Niu, H. Zhang, B. Yang, D. Ebeling, J. Tschakert, T. Cheng, A. Schirmeisen, A. Narita, K. Müllen, L. Chi, *J. Am. Chem. Soc.* **2019**, *141*, 7399–7406.
[13] a) T. Mori, *Chem. Rev.* **2021**, *121*, 2373–2412; b) A. Tsurusaki, K. Kamikawa, *Chem. Lett.* **2021**, *50*, 1913–1932.
[14] N. B. Chen, B. Yan, *Molecules* **2018**, *23*, 3376.
[15] V. Kiran, S. P. Mathew, S. R. Cohen, I. H. Delgado, J. Lacour, R. Naaman, *Adv. Mater.* **2016**, *28*, 1957–1962.
[16] Y. Shen, C.-F. Chen, *Chem. Rev.* **2012**, *112*, 1463–1535.
[17] a) P. Ravat, *Chem. Eur. J.* **2021**, *27*, 3957–3967; b) C. Goedicke, H. Stegemeyer, *Tetrahedron Lett.* **1970**, *11*, 937–940; c) X. L. Yao, W. H. Zheng, S. Osella, Z. J. Qiu, S. Fu, D. Schollmeyer, B. Müller, D. Beljonne, M. Bonn, H. I. Wang, K. Müllen, A. Narita, *J. Am. Chem. Soc.* **2021**, *143*, 5654–5658; d) S. Ma, J. J. Gu, C. J. Lin, Z. X. Luo, Y. P. Zhu, J. B. Wang, *J. Am. Chem. Soc.* **2020**, *142*, 16887–16893.
[18] a) J. M. Fernández-García, P. Izquierdo-García, M. Buendía, S. Filippone, N. Martín, *Chem. Commun.* **2022**, *58*, 2634–2645; b) C. Shen, G. Zhang, Y. Ding, N. Yang, F. Gan, J. Crassous, H. Qiu, *Nat. Commun.* **2021**, *12*, 2786; c) Y. Zhu, Z. Xia, Z. Cai, Z. Yuan, N. Jiang, T. Li, Y. Wang, X. Guo, Z. Li, S. Ma, D. Zhong, Y. Li, J. Wang, *J. Am. Chem. Soc.* **2018**, *140*, 4222–4226; d) Y. Chen, C. J. Lin, Z. X. Luo, Z. B. Yin, H. N. Shi, Y. P. Zhu, J. B. Wang, *Angew. Chem. Int. Ed.* **2021**, *60*, 7796–7801; *Angew. Chem.* **2021**, *133*, 7875–7880; e) H. Shi, B. Xiong, Y. Chen, C. Lin, J. Gu, Y. Zhu, J. Wang, *Chin. Chem. Lett.* **2023**, *34*, 107520.
[19] a) N. J. Schuster, R. Hernández Sánchez, D. Bukharina, N. A. Kotov, N. Berova, F. Ng, M. L. Steigerwald, C. Nuckolls, *J. Am. Chem. Soc.* **2018**, *140*, 6235–6239; b) B. Liu, M. Böckmann, W. Jiang, N. L. Doltsinis, Z. Wang, *J. Am. Chem. Soc.* **2020**, *142*, 7092–7099; c) X. Xiao, S. K. Pedersen, D. Aranda, J. Yang, R. A. Wiscons, M. Pittelkow, M. L. Steigerwald, F. Santoro, N. J. Schuster, C. Nuckolls, *J. Am. Chem. Soc.* **2021**, *143*, 983–991; d) Z. Qiu, C.-W. Ju, L. Frédéric, Y. Hu, D. Schollmeyer, G. Pieters, K. Müllen, A. Narita, *J. Am. Chem. Soc.* **2021**, *143*, 4661–4667.
[20] a) S. H. Pun, K. M. Cheung, D. Y. Yang, H. Chen, Y. J. Wang, S. V. Kershaw, Q. Miao, *Angew. Chem. Int. Ed.* **2022**, *61*, e202113203; *Angew. Chem.* **2022**, *134*, e202113203; b) Y. Nakakuki, T. Hirose, H. Sotome, M. Gao, D. Shimizu, R. J. Li, J. Y. Hasegawa, H. Miyasaka, K. Matsuda, *Nat. Commun.* **2022**, *13*, 1475.
[21] F.-L. Zhang, K. Hong, T.-J. Li, H. Park, J.-Q. Yu, *Science* **2016**, *351*, 252–256.
[22] Deposition Numbers 2206392 contain the supplementary crystallographic data for this paper. These data are provided free of charge by the joint Cambridge Crystallographic Data Centre and Fachinformationszentrum Karlsruhe Access Structures service.
[23] Z. F. Chen, C. S. Wannere, C. Corminboeuf, R. Puchta, P. V. Schleyer, *Chem. Rev.* **2005**, *105*, 3842–3888.
[24] D. Geuenich, K. Hess, F. Köhler, R. Herges, *Chem. Rev.* **2005**, *105*, 3758–3772.
[25] a) H. Tanaka, M. Ikenosako, Y. Kato, M. Fujiki, Y. Inoue, T. Mori, *Commun. Chem.* **2018**, *1*, 38; b) J. K. Li, X. Y. Chen, Y. L. Guo, X. C. Wang, A. C. H. Sue, X. Y. Cao, X. Y. Wang, *J. Am. Chem. Soc.* **2021**, *143*, 17958–17963.
[26] G. M. Paternò, Q. Chen, R. Muñoz-Mármol, M. Guizzardi, V. Bonal, R. Kabe, A. J. Barker, P. G. Boj, S. Chatterjee, Y. Ie, J. M. Villalvilla, J. A. Quintana, F. Scotognella, K. Müllen, M. A. Díaz-García, A. Narita, G. Lanzani, *Mater. Horiz.* **2022**, *9*, 393–402.
[27] R. Englman, J. Jortner, *Mol. Phys.* **1970**, *18*, 145–164.

Manuscript received: December 12, 2022
Accepted manuscript online: February 1, 2023
Version of record online: February 20, 2023